Nanoscale

Accepted Manuscript

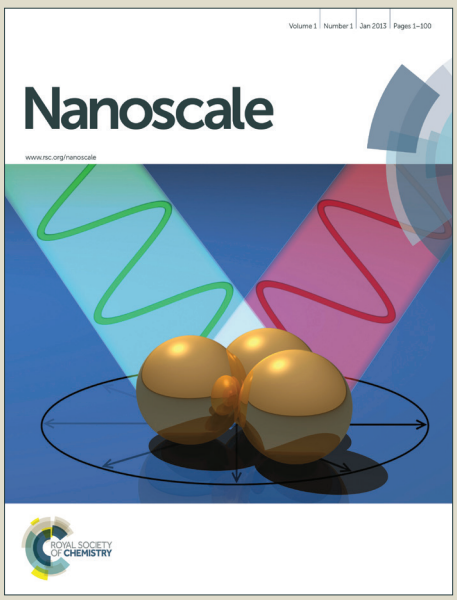

ROYAL SOCIETY OF CHEMISTRY

www.rsc.org/nanoscale

Table of Contents

Microwave assisted synthesis of carbon dots and their direct involvement in whole chain electron transfer processes, yielding augmentation in photosynthesis.

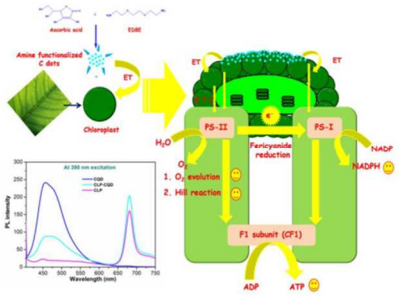

Cite this: DOI: 10.1039/c0xx00000x

www.rsc.org/xxxxxx

ARTICLE TYPE

High throughput electron transfer from carbon dots to chloroplast: A rationale of enhanced photosynthesis

Sourov Chandra*[a], Saheli Pradhan[a], Shouvik Mitra[a], Prasun Patra[a], Ankita Bhattacharya[a], Panchanan Pramanik[b], Arunava Goswami[a]

Received (in XXX, XXX) Xth XXXXXXXXX 20XX, Accepted Xth XXXXXXXXX 20XX
DOI: 10.1039/b000000x

A biocompatible amine functionalized fluorescent carbon dots have been developed and isolated for gram scale applications. Such carbogenic quantum dots can strongly conjugated over the surface of the chloroplast and due to that strong interaction the former can easily transfer electrons towards the latter one by assistance of absorbed light or photons. An exceptionally high electron transfer from carbon dots to the chloroplast can directly effect on the whole chain electron transfer pathway in light reaction of photosynthesis, where electron carriers plays important role in modulating the system. As a result, carbon dots can promote photosynthesis by modulating the electron transfer process as they are capable to fasten the conversion of light energy to the electrical energy and finally to the chemical energy as assimilatory power (ATP and NADPH).

Introduction

Chemistry and biology has been intrinsically related to each other since the evolution of life, a wide variety of natural system displays this artefact quite clearly. As for example life has been cycled by harvesting sunlight to energy by means of photosynthesis through a large number of complex steps that are involved in to it. Photosynthesis is mostly carried out by plants and algae, but some typical photosynthetic bacteria are also capable of doing so. [1] They absorb sunlight and convert them in the form of electrochemical energy. [2] Interestingly chromophores such as chlorophylls and xanthophylls are present on the thylakoid membrane of chloroplast which acts as antenna during photosynthesis. [3] Chromophoric constituents assembled in protein structure are merely known as light harvesting complex. They absorbs energy and then transports to photosystem I and II followed by a series of electron transfer processes, which ultimately produce the oxygen and ATP by means of water splitting along with the reduction of NADP to NADPH. [4] A lot of efforts have been paid to enhance the photosynthetic efficiency [5] by using luminescence effect of quantum dots [6] or Plasmon enhancement effect of gold and silver nanoparticles and nanoshells. [7] To address this issue here in we propose a carbon dot based electron transfer (ET) approach to augment the light cycle pathways in photosynthesis for the first time.

Quantum dots (QDs), a zero dimensional nanostructure, of late found its versatile applications in devising exclusive platform for bio-sensing, light/energy harvesting applications, rapid detection and energy transfer processes with their high luminescence and unique photophysical properties. [8-10] Classical heavy metal QDs such as ZnS, ZnSe, CdS, CdSe, CdTe or mixed heavy metal QDs are widely used for electron transfer processes so far, [11] however from biological perspectives they are expected to give rise undesired toxicity within the system. [12] By virtue multiple nano-light emitter carbon dots are now under the limelight as a suitable alternatives of the heavy metal QDs with their λ_{ex} dependent photoluminescence (PL) properties, high PL quantum yield, high photostability without photobleaching, large two-photon excitation cross-sections and obviously its non-toxicity. [13-16] Elegantly carbon quantum dots (CQDs) are now being used in bioimaging, biosensing, detection and photovoltaic applications. [13, 14, 17] Quite a few techniques are involved to synthesize CQDs which includes laser ablation, [18] electro-oxidation, [19] microwave irradiation, [20] solvothermal or pyrolytic degradation [21, 22] and hot solvent injection. [23] CQDs are known as good electron donor as well as acceptor, [24] which lead to various opportunities on light energy conversion, light emitting diodes, photoreduction and related photocatalytic reactions. [13, 14] However, a very few works have been done on CQDs based light stimulated electron transfer process on photosynthetic system/light harvesting complex [25] and hence it is still unresolved till date.

Here in we propose a simple microwave assisted synthesis of amine terminated CQDs with a high quantum yield (QY) of 4.5% without external passivation and augmentation of photosynthesis by electron transfer from CQDs-donor to chloroplast-acceptor. As

[a] *AERU, Biological Sciences Division, Indian Statistical Institute, Kolkata, 700108, India.*
E.mail: chandrasourov@gmail.com
[b] *Nanomaterials laboratory, Department of Chemistry, Indian Institute of Technology Kharagpur, Kharagpur, 721302, India.*
† Electronic Supplementary Information (ESI) available: See DOI: 10.1039/b000000x/

both can absorb at the same wavelength region with partial overlapping of emission spectra for CQDs with absorption spectra of chloroplast, the former can easily transfer its electron towards the latter one by absorption of light. Remarkably high electron transfer efficiency has been observed from CQDs to chloroplast which corroborates with the series of complex electron transfer reaction that are involved in light cycle pathways. Elevated oxygen evolution, ATP formation, NADP reduction and higher Hill reaction enlightens the above mentioned ET process. Though a few ET experiments have been carried out on photosynthesis, [26] but this report is in fact the first one to claim the CQDs based ET on photosynthetic system and its correlation affecting the total light cycle pathway.

Experimental

Materials

Ascorbic acid, mannitol and EDTA were purchased from Sisco Research Laboratory (SRL), whereas 2,2-(ethylenedioxy)bis(ethylamine) (EDBE), 2,6-dichlorophenol indophenol (DCPIP), NaCN, sucrose, 4-(2-Hydroxyethyl) piperazine-1-ethanesulfonic acid, N-(2-Hydroxyethyl) piperazine-N′-(2-ethanesulfonic acid) (HEPES), $MgCl_2$, NH_4Cl, NaN_3, ferricyanide, tricine, K_2HPO_4, ADP, trichloroacetic acid, spinach ferredoxin and NADP were received from Sigma Aldrich. BSA and NaOH were obtained from Merck (India).

Synthesis of amine functionalized carbon quantum dots

300 mg ascorbic acid was dissolved in 10 mL of water, 200 µL of EDBE was added to it; after well mixing the solution was put into a microwave oven. Heating was then performed at 450 Watt in which the colourless solution turned to brown in colour. Excess EDBE was removed though dissolving the product into water and then separating with excess acetone. Finally the above solution was decanted and the product was dried in a vaccum oven at 80°C for 24 hours. The resulting carbon dots were well dispersed in water.

Isolation of chloroplast

Young and fully expanded deveined mung bean leaves were ground with blender in a medium containing mannitol, HEPES, EDTA, $MgCl_2$ and BSA in ice cold condition. In brief, the leaves were homogenized in chloroplast isolation buffer containing 330 mM mannitol, 30 mM HEPES, 2 mM EDTA, 3mM $MgCl_2$ and 0.1% w/v BSA (pH7.8) using blender for 15 sec. The slurry was filtered through 8-layers of cheese cloth followed by centrifugation at 250g for 5mins.The supernatant was again centrifuged at 1000g for another 5min. The chloroplast was washed and resuspended in extraction buffer and used for tracking photosynthetic pathway.

Electron transfer (ET) Study

ET was evaluated by the dropwise addition of chloroplast and chlorophyll separately into a constant concentration of carbon dots. Chloroplast suspension was prepared by mixing of chloroplast in a buffer containing 100 µM phosphate buffer (pH 7.8), 2 µM NaCN and 1.25 mM sucrose. 50 µL of chloroplast having concentration of 378.45µg/mL was gradually added to 2.5 mL 1:1 aqueous-buffer solution of CQD. Similarly chlorophyll (1.047 µg/mL) dissolved in acetone was gradually added to the CQD solution and after that the change in PL intensity was monitored by PL spectrophotometer.

Whole chain electron transport

The electron transport through the whole chain of photosynthesis, i.e. from water to methyl viologen (MV) (oxygen uptake) was measured polarographically with an Oxygraph oxygen electrode (Hansatech Instruments, UK). Assay medium (3 mL) consisted of 50mM HEPES (pH 7.5), 10 mM NaCl, 1 mM NH_4Cl, 3 mM $MgCl_2$, 1.0 mM NaN_3, and 0.5 mM MV. Chloroplast was added to the above reaction mixture to a total concentration of 378µg/mL.

Oxygen evolution measurement

Oxygen evolution was assayed in a medium containing 378.45µg/mL of chloroplasts. The 2.9mL assay medium consisted of sorbitol, 0.33 M; NaEDTA, 2.0 mM; $MgCl_2$, 1.0 mM and HEPES, 50 mM, adjusted to pH 7.6 at 20° C with NaOH. Sodium 2,6-dichlorophenolindophenol, 0.88 mM, served as oxidant in all assays and was added to the medium immediately prior to injection of the chloroplasts. The isolated CLP were illuminated for 1 min with 500 µmol m^{-2} s^{-1} visible light (400–700 nm) and ultraviolet light (300–340 nm) illumination, respectively, then the assays of photochemistry reaction were carried out.

Hill reaction in chloroplast

Hill activity was assayed according to the method of Vishniac (1957). Fresh leaves were extracted in sucrose-phosphate buffer (0.4M sucrose in 0.05M phosphate buffer) at pH 6.2 and centrifuged at 1000g for 5mins. The pellet was discarded and supernatant was collected. The supernatant was centrifuged at 5000g for 15mins. The pellet containing chloroplasts was taken and sucrose-phosphate buffer was added to it to make the volume 5ml. 1ml chloroplast suspension, 4ml sucrose-phosphate buffer and 0.5ml 0.03% 2,6-dichlorophenolindophenol (DCPIP) were added in a test tube and initial absorbance was recorded at 610 nm. After 5minutes of saturating radiance, optical density values were again measured at 610nm. Hill activity was expressed as µmole DCPIP reduced per hour per mg chlorophyll.

Photophosphorylation

Ferricyanide and NADP reduction were determined by the spectrophotometric methods of Trebst. Ferricyanide reduction was measured using a mixture (1.45 ml) containing chloroplasts (378.45µg/mL); 86 mm sorbitol, 50 mM Tricine (pH 8.1), 50 mM NaCl, 5 mM $MgCl_2$, 2 mM K_2HPO_4, 2 mm ADP, and 1 mm ferricyanide. Immediately following 1 min of saturating irradiance, trichloroacetic acid was added to a final concentration of 2%. Chloroplasts were pelleted by centrifugation and the absorbance of the supernatant determined at 420 nm. Dark controls showed no ferricyanide reduction. The experimental conditions for measuring NADP reduction were identical except for the deletion of ferricyanide from the reaction medium and the addition of 3 µM purified spinach ferredoxin (Sigma) and 0.66 mM NADP. After 1 min of irradiance the reaction mixture was centrifuged and determined at 340 nm.

ATP synthesis measurement

Light-induced ATP synthesis of chloroplasts was measured by comparing the ATP level in the dark and 1 min after illumination. One-milliliter reaction mixture contained 0.4 M sucrose, 50 mM Tris-HCl (pH 7.6), 10 mM NaCl, 5 mM $MgCl_2$, 2mM ADP, 10 mM Na_2HPO_4, and intact chloroplasts (378.45µg/mL). After illumination for 1 min, 10% TCA was immediately added to the illuminated and dark-controlled samples and neutralized with 3M Na_2CO_3. ATP content was then analyzed by Biovision ATP Colorimetric/Fluorometric Assay Kit.

MTT assay

MTT [3-(4, 5-dimethylthiazol-2-yl)-2,5-diphenyltetrazolium bromide] assays were performed on human breast carcinoma HBL-100 cell lines and the cell viability was recorded after exposure to CQDs at different concentrations up to 24 hrs. Cells were seeded into 96-well microtiter plates at a density of 5×10^5 per well and allowed to adhere for 24 hrs. Then CQDs were introduced at two different concentrations of 100 µg/mL and 200 µg/mL. After incubation, cells were washed with PBS twice and incubated with MTT solution (450µg/ml) for 3-4 hrs at 37^oC. The resulting formazan crystals were dissolved in an MTT solubilization buffer and the absorbance were measured at 570 nm by using a microplate reader (Biorad) and the values were compared to the control cells.

Evaluation of in vivo toxicity: blood biochemical parameters and histopathological analysis

Healthy young, non-pregnant, nulliparous swiss albino mice, weighting about 20–22 g (8 weeks old) were placed in clean polypropylene cages with access to food and water. These cages were maintained in an air-conditioned animal house at 20–28^oC, 50–70% relative humidity and 12 h light–dark cycle. The animals were provided with commercial mice pellet diet and deionized water. After one week acclimation, the mice were randomly divided into 3 groups, each group consisted of five female and five male mice. They were kept separately in polypropylene cages. Two doses 100 µg mL^{-1} and 200 µg mL^{-1}, were selected for amine functionalized CQD treatment. CQDs were suspended in water and dispersed by sonication for 15 min before treatment. Toxicity of that carbon dots were evaluated by intravenous injection pathway through tail vein. 100 µL of CQD with maximum concentration 100 µg mL^{-1} and 200 µg mL^{-1} was injected through tail vein and the animals were sacrificed after 7 days of injection. Blood and serum were collected and major organs such as brain, heart, lung, liver, spleen, stomach, kidneys, testis or uterus were dissected out.

Characterization techniques

Fourier Transform Infrared Spectroscopy (FTIR) was conducted by Perkin-Elmer spectrum 2 FTIR spectrophotometer. For absorption and fluorescence measurements we have used PerkinElmer spectrophotometer (model no: LAMDA 25) and spectrofluorimeter (model no: LS55), respectively. Phase characterization was carried out by X-ray diffractometer (XRD; model no. PW1710). Sample for XRD was prepared by the deposition of well dispersed carbon dots on glass slide and after drying the analysis was performed by using copper as the target material. High resolution transmission electron microscopy (HR-TEM) and Energy dispersive X-ray (EDX) analysis were carried out by using JEOL JEM 2010, operating at an acceleration voltage of 200 kV. In HR-TEM analysis a very dilute aqueous suspension was prepared, which was then deposited on a copper grid and finally dried in air. The X-ray photoelectron spectroscopic (XPS) data was collected using an Al Ka excitation source in an ESCA-2000 Multilab apparatus (VG microtech). Zeta potentials were measured by using Malvern zetasizer while Time Correlated Single Photon Counting (TCSPC) lifetime measurement was carried out by using a picosecond diode laser at 370 nm (IBH, Nanoled) as a light source and the signal was taken at magic angle (54.7^o) polarization using a Hamamatsu MCP PMT (3809U). The data analysis was evaluated by using IBH DAS, version 6, and decay analysis software. TEM (JEOL JEM 2010) and FE-SEM (JEOL JSM-6340F) of treated and untreated chloroplast were performed in order to understand the interaction between chloroplast and CQDs in photosynthesis. Both treated and non treated chloroplast were illuminated for 1minute and centrifuged at 1000g for 5min .The chloroplasts were fixed in formaldehyde-glutaraldehyde containing 7% sucrose. After washing in 0.1 M phosphate buffer (pH 7.2) containing 7% sucrose, the tissue was post fixed for 2 hr in 1% OsO_4, washed and dehydrated through a graded series of alcohol, and examined under microscope.

Results and discussions

Energy conversion and storage has been a basic triumph for evolution of life as has been noticed from ancient times. Chemists have been trying to adopt natural resources by artificial miniaturization. Here in we propose a simple chemistry to rationale photosynthesis by means of electron transfer from carbon dots to the chloroplast; the whole process is summarized

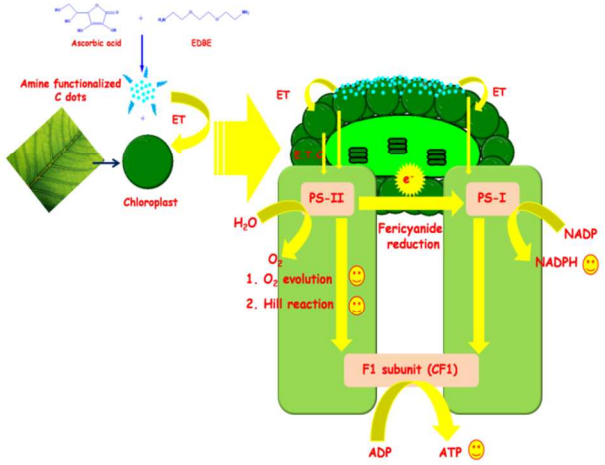

Scheme 1 Schematic representation illustrating the whole process.

in scheme 1. Amine functionalized carbon quantum dots (CQDs) were synthesized by a simple microwave assisted process using ascorbic acid and EDBE as the precursor. CQDs exhibited high luminescence property without any further passivation and acted as an electron donor after conjugation with chloroplast (CLP). Such excess electrons received by CLP was then transported to photosystem II (PS-II) and photosystem I (PS-I) and thereby

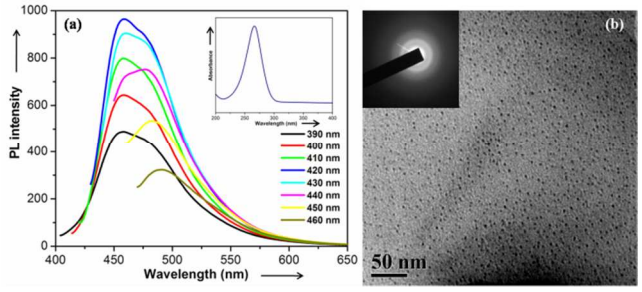

Fig. 1 (a) PL spectra of CQDs at different excitation wavelength, inset: UV-Vis absorbance spectra of CQDs; (b) TEM image of CQDs, inset: corresponding SAED pattern.

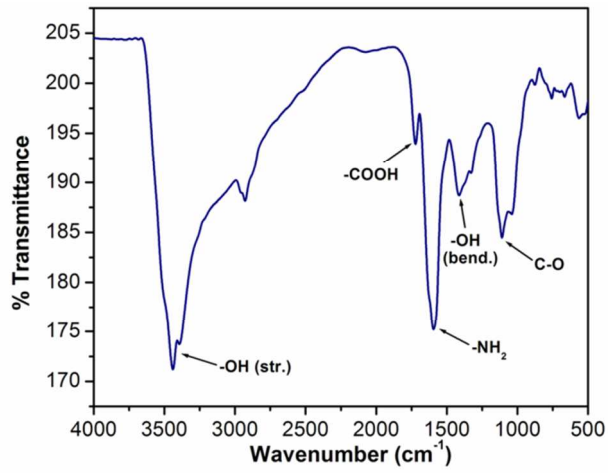

Fig. 2 FTIR spectrum of the C-dots.

increasing the total electron transport chain (ETC) in photosynthesis. As a result the total light cycle pathway involved in PS-I and PS-II was extended with increasing the splitting of water to O_2, NADP reduction and ATP formation.

Large scale synthesis of CQDs and its isolation in its pure form had been a really tough task to execute; especially a small amount of CQDs in its pure form could only be isolated through running a gel electrophoresis technique. [27] In that aspect our process demanded a high throughput facile synthesis of carbon dots into its pure form yielding about ~61.5 mg of product from a single synthetic step. A digital photograph of the isolated CQDs was represented in figure S1. As synthesized CQDs exhibited strong absorption spectra at 266 nm (figure 1a inset), which is similar to the other carbogenic quantum dots reported earlier. [13, 14] CQDs were luminescent in nature and exhibited blue luminescence under the exposure of UV light. PL spectra of CQDs were recorded at different excitation wavelength starting from 390 nm to 460 nm shown in figure 1a; a gradual red shifted pattern in the emission spectra was noted with different excitation wavelength from 390 to 460 nm while maximum PL intensity was observed at 420 nm excitation. Corresponding normalized PL spectra was illustrated in figure S2. This result in fact was consistent with the earlier observations where CQDs exhibited excitation dependant emission pattern. [13] TEM image shown in figure 1b confirmed the presence of very small sized absolutely spherical carbon dots while SAED pattern forecasted its poor crystallinity. The corresponding HR-TEM image (figure S3) was also represented the particle uniformity with average particle size of 1-2 nm. Such amorphous nature was further confirmed from XRD pattern (figure S4), which indexed [002] plane of carbon with a single broad peak at $2\theta = 22.8^0$. [28]

Surface functionality of CQDs was evaluated by FTIR spectra (figure 2), affirming the presence of –OH, $–NH_2$ and C–O groups as the peaks centred at 3445 (–OH stretching), 1417 (–OH bending); 1593 and 1111 cm^{-1} respectively. [21, 29] A weak but sharp peak at 1723 cm^{-1} was assigned to a little amount of carboxylic acid present on the surface of CQDs. EDX spectrum validated the presence of C, O and N as the main chemical components of CQDs (figure S5), which again correlated with its amine functionality. Finally the result obtained from XPS analysis (figure S6) confirmed the existences of C, N and O as the peaks were centred at 284.8 (C 1s), 400 (N 1s) and 531 eV (O 1s) respectively. [30, 31] When we checked the zeta potential of CQDs at different pH, a stable dispersion with a positive zeta potential at acidic pH (1 to 6) was noted. It became negative at around pH 7 and such negative value increased with increasing the pH, followed by its saturation at pH 10 (figure S7). The positive potential at low pH might be due to the formation of $–NH_3^+$; [22, 32] while the residual carboxylic acid groups were deprotonated producing $–COO^–$ ions responsible for their negative zeta potential at around pH 7. Even amine itself could show negative potential at pH > 7 owing to the formation of negatively charged Stern layer over their positive charged surface. [32, 33] Similar trend was also followed on verifying the PL emission of CQDs against pH of the medium, which demonstrated that PL intensity was increased with lowering the pH of the solution and attained maximum at pH 1 (figure S8). Such phenomena might be explained by conversion of $–NH_2$ groups to $–NH_3^+$ at acidic pH, resulting minimum aggregation and hence elevated its PL property. [17, 34] Worthwhile a high quantum yield of 4.5% was observed at 420 nm excitation at pH 7 with respect to quinine sulphate chosen as standard. It was speculated that radiative recombination of excitons, emissive traps, free zig-zag sites, quantum confinement and defect sites during incorporation of functionality were responsible for such high PL properties. [13, 14, 35] Partial passivation by EDBE chain to the carbon core formed by ascorbic acid during synthesis might contribute to high PL property as well. [17, 18] Such CQDs showed brilliant photostability under photo irradiation conditions for 8 h without exhibiting photo bleaching property (figure S9). [15] All together CQDs were quite stable without photobleaching and exhibited high QY at acidic pH with small particle size distribution.

We chose CQDs to pair with CLPs since they can absorb light in the same wavelength region and hence a single wavelength could able to excite both of them and boost electrons from carbon dots to chloroplast and also chloroplast to the photosystem. Figure 3a demonstrated the overlapped spectral pattern of CQDs and CLPs; CLPs exhibited a strong absorbance within 400-550 nm therefore its shoulder overlapped significantly with emission pattern of CQDs at 390 nm excitation wavelength. Figure 3b displayed the PL spectral pattern of the individual CQD and CLP along with the mixture of CQD and CLP at 390nm excitation. It was evident that the emission maxima of CQDs was decreased at 456 nm while emission maxima resembled to that of CLPs was

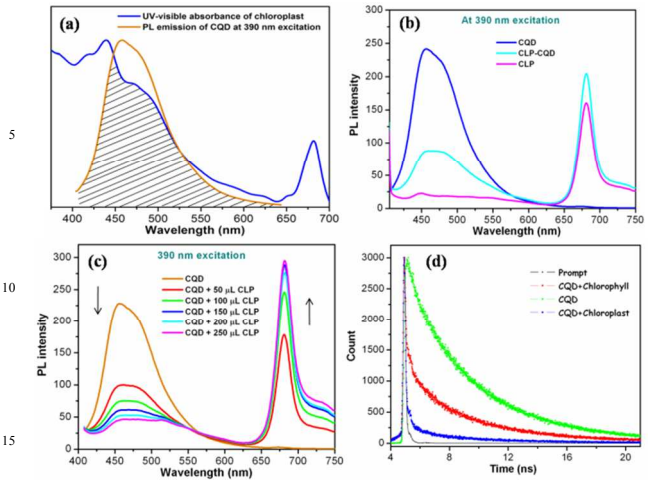

Fig. 3 (a) Merged area for the spectral overlap of the normalized PL-emission of CQDs at 390 nm excitation with the UV-Vis absorbance of the chloroplast; (b) PL spectra of CQD, chloroplast and the mixture of CQD and chloroplast at 390 nm excitation; (c) PL intensity of CQD with dropwise addition of CLP under 390 nm excitation; (d) PL life time decay profile of CQD, CQD+CLP and CQD+CP.

increased at 681.5 nm by virtue of their strong interaction in their mixed condition. Similar phenomena were also observed at 420 and 442 nm excitations shown in figure S10 and S11 respectively. Such enhancement of acceptor emission signal might be due to the direct absorption of the emitted photons from the CQDs, therefore it might be a radiative excitation. Furthermore, with gradual addition of CLPs into a solution of carbon dots at 390 nm excitation, a gradual quenching in emission spectra of CQDs at 456 nm were noted (figure 3c) through energy transfer from CQDs to CLPs with formation of a stable assembly. Again the simultaneous PL enhancement for CLPs at 681.5 nm might be due to the introduction of more numbers of CLPs into the solution along with the excited energy transfer from CQDs to CLPs. [36] It was apparent that after addition of certain amount of CLPs (378.45µg/mL), the emission of CQD was almost disappeared indicating the complete electron or energy transfer from donor (CQDs) to acceptor (CLPs). If the LUMO of CQDs was above the LUMO of chloroplast, then emission quenching and life time decrease were induced by electron transfer from CQDs to chloroplast; which seems to be the case here. [37] This experiment was again repeated at two other excitations, 420 nm and 442 nm respectively (figure S12 and S13), where analogous gesture was reported to that of the 390 nm excitation. It was again repeated for chlorophyll, as it is the major pigment of chloroplast; the outcome was identical to that one carried out for CLPs (figure S14 and S15). The life time of CQD was astonishingly decreased after conjugation of both CLP and CP. The decay profile shown in figure 2d represented that whether CQD had a long life time of 4.16 ns, after addition of CLP and CP, it was reached to 0.08 and 0.49 ns respectively. Such result also corroborated with the quenching as discussed above. A plot of ET efficiency against the ratio of CLPs : CQDs at different excitation wavelength (figure S16) revealed that the maximum ET efficiency was observed at 442 nm excitation with approximate 93% electron transfer from CQDs to CLPs when the ratio of CLPs : CQDs reached at 0.35. Nearly 84% and 74% ET efficiency at 420 and390 nm excitation was noted at that particular ratio.

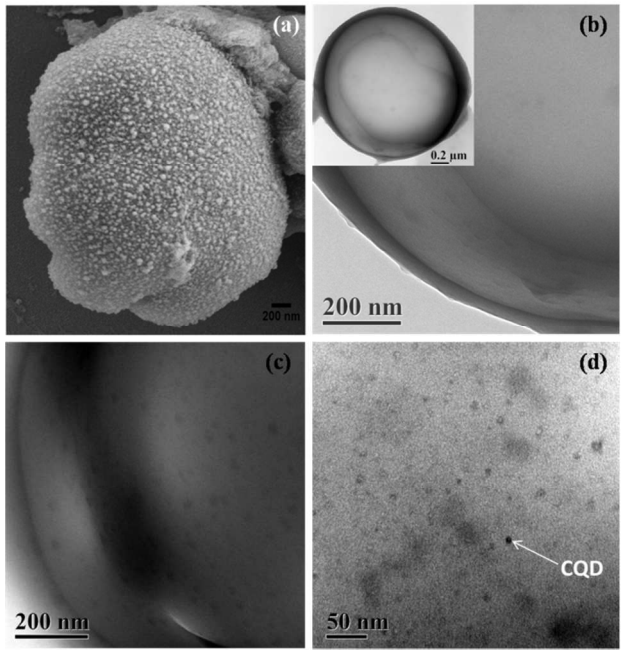

Fig. 4 (a) FESEM image of CQD treated CLP. (b) TEM image of untreated CLP, (c) TEM and (d) corresponding HR-TEM image CLP after treatment with CQDs. The inset in figure b is the low resolution image of the CLP.

The huge electron transfer from CQDs to CLPs might be explained by the close proximity between donor and acceptor respectively which was resulted during the adsorption of CQDs on to the large surface of CLPs and form a light harvesting complex. The standard curve signifying absorbance against concentration of CQDs (figure S17), elucidated that nearly 2.74µg of CQDs was adsorbed on per micro gram of CLPs (detailed in supporting information). This adsorption of CQDs on to CLPs surface ensued a close distance followed by a very strong overlapping absorption spectral pattern of donor-acceptor as mentioned earlier allowed remarkably high electron transfer efficiency. The formation of a CQD-CLP assembly was confirmed by fluorescence life time decay profile measurements as mentioned earlier. Though CQDs exhibited bi-exponential fluorescence decay with average life time of 4.16 ns, [38] however after addition of CLPs the life time of CQDs were drastically dropped to 0.08 ns at CLPs: CQDs ratio of 0.35 (figure 3d). Several microscopic techniques were further used to ensure that above speculation. Figure 4a exhibited FE-SEM image of the CQD treated CLP, illustrating the distribution of CQDs over the surfaces of CLPs; moreover the membrane of CLPs was unperturbed in post treated condition. Similarly figure 4b and 4c represented the TEM images of the untreated and the treated CLP. The corresponding HRTEM image was shown in figure 4d, by which it was clearly evident that after treatment the surface of CLP was completely covered by the CQDs. Although the CQDs underwent some sort of aggregation in treated sets which was expected during interaction/internalization with/within biological systems. [39] Figure 4d again confirmed the presence of high dense particles throughout its surface. Interestingly in post treated environment the regular morphology of CLP was restored and

remained intact without any distortion.

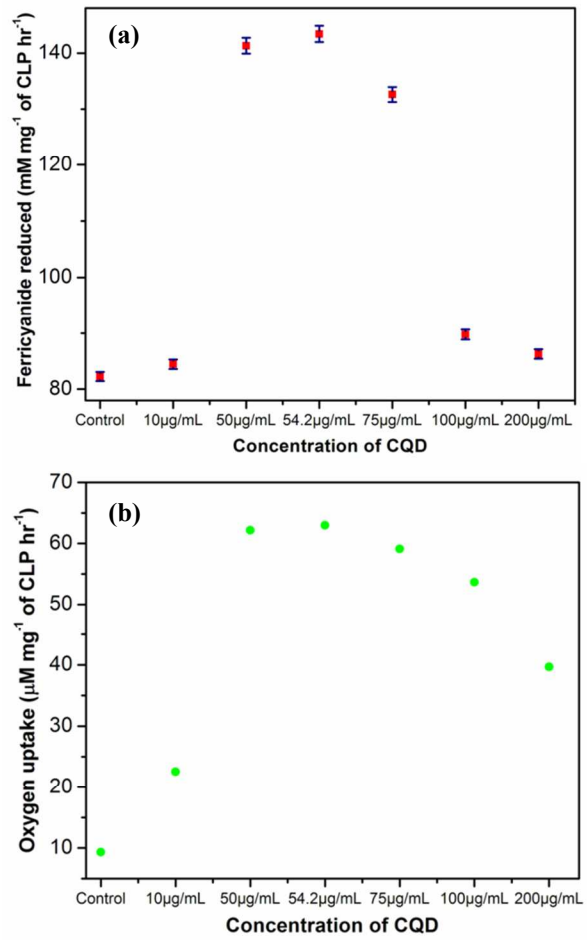

Fig. 5 (a) Effect of CQD on ferricyanide reduction and (b) plot of oxygen uptake against the concentration of CQD.

Therefore the electron transfer from CQDs to CLPs ensemble the excess electrons to the light harvesting system and hence additional information were required at this stage to recognize fate of the transferred electrons. To identify the underlying electron transfer process we carried out the reactions which were involved in photophosphorylation activity of both PS-I and PS-II in presence of different artificial electron acceptors. It is well known that isolated chloroplast liberates oxygen in presence of ferricyanide, where reduction of ferricyanide occurs by electron transfer from PS-II. [40] Figure 5a showed the results of ferricyanide reduction in presence and absence of CQDs which was an indicator of ET process; [41] quite interestingly higher ferricyanide reductions were obtained in all the CQD treated samples. Maximum reduction was obtained at the concentration of 54.2µg/mL of CQDs pointing 74.3% additional reduction of ferricyanide in contrast to the control samples, which confirmed the large amount of electron transfer from the reaction centre to PS-II in presence of CQDs. Therefore ferricyanide reduction assay with control and treated chloroplasts confirmed the better activity of PS-II in presence of carbon dots, signifying augmentation in photosynthesis as well as ET process between CQDs and CLPs. The electron transport chain (ETC) through oxygen uptake study was shown in figure 5b revealed that CQD

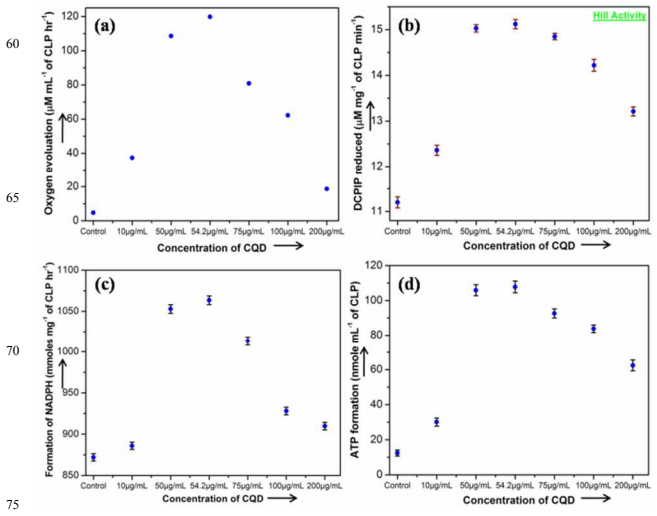

Fig. 6 Effect of CQD on (a) oxygen evaluation, (b) Hill activity by DCPIP reduction, (c) conversion of NADP to NADPH and (d) the formation of ATP.

conjugated CLP exposed the maximum of ~6.7 times higher uptake as respect to the control one, which again followed the similar trend as discussed earlier for ferricyanide reduction. Therefore CQD-CLP assembly should assured high photosynthetic activity even at much lower concentration. As oxygen evolution was the by-product of the photosynthesis, estimation of oxygen evolution was necessary at this stage to correlate the activity of ETC. DCPIP (2,6-dichlorophenol indophenol), a strong electron acceptor was used to measure the oxygen evolution polarographically (figure 6a). [41] Highest oxygen evolution was recorded at 54.2µg/mL concentration of CQDs; beyond that concentration oxygen evolution was gradually decreased. Hill reaction, an alternative method of polarography was frequently checked in terms of Hill activity measurement using the same electron acceptor, DCPIP (figure 6b). [42] The reduction of DCPIP was directly proportional to the amount of oxygen evolved during the electron transfer process in photosynthesis. In Hill activity, a maximum of 26% higher reduction of DCPIP was observed in contrast to the control at the optimal concentration (54.2µg/mL) of CQDs. Therefore the energy or electron transferred from CQD to CLP influenced the whole PS-II. The influence of CQDs on PS-I after ET was evaluated using another strong electron acceptor NADP. [41] In presence of CQDs the conversion of NADP to NADPH was further fastened (figure 6c), confirming more electrons were transferred from PS-II to PS-I or directly from CP to PS-I. Analogous to all above observations, the reduction of NADP at any concentration of CQDs were higher and 191.52 mmoles of excess NADPH was produced in an hour using per mg of CLP with respect to the control at that optimum aforementioned concentration of CQDs. Final step in light cycle pathway was the generation of ATP, which was utilized in carbon assimilation by "dark biochemistry" in photosynthesis where more ATP production signified more photophosphorylation activity of ETC. [43] Ultimately the same trend was also found in the final step where ~8.7 times more ATP was generated at the optimum concentration of CQDs with respect to the control one (figure 6d). Therefore it was concluded that CQDs at first transferred the

excess electrons to CP by absorption of light and such intemperance electrons never went on futile. The associated biochemical reactions justified that transferred energy sharpened the subsequent electron transfer in light cycle pathways there by giving rise to higher ATP and NADPH formation thus modulating photosynthesis.

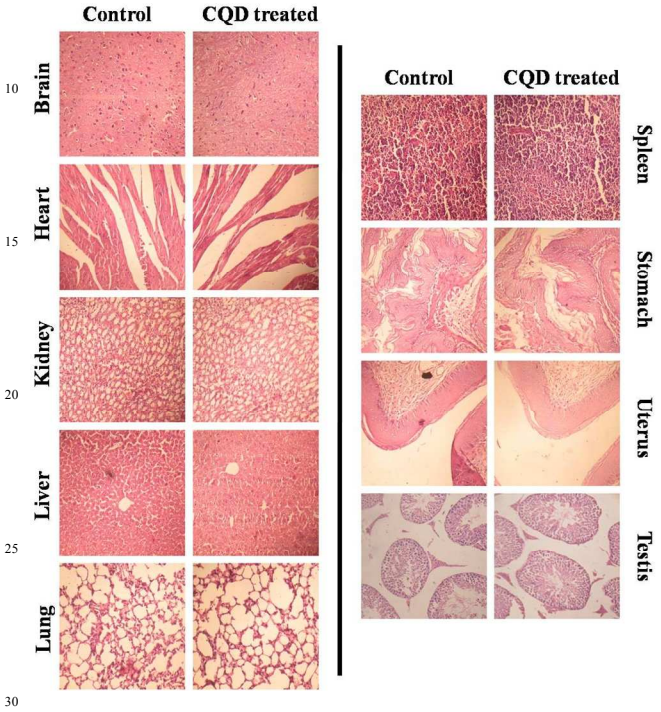

Fig. 7 Histopathological analysis of major organs such as brain, heart, kidney, liver, lung, spleen, stomach, uterus and testis of control mice and CQD (200 µg/mL) intravenously injected mice. No significant difference between control and treated mice was observed.

Finally we carried out *in vitro* and *in vivo* analysis to determine the toxicity of CQDs for biological perspectives. Non-toxicity and biocompatibility of CQDs were ensured by MTT assay on HBL-100 breast carcinoma cell line with ~90% viable cells were present at the highest concentration (200µg/mL) of CQDs (figure S18). [15] For *in vivo* toxicity determination two aforementioned concentrations of CQDs were injected to healthy nulliparous swiss albino mice through tail vein. The mice were healthy without any abnormality and blood and serum biochemical parameters were tested. No significant alterations were observed either in hematology markers such as RBC, WBC, neutrophils, basophils, lymphocytes, monocytes, eosinophils and platelet counts nor in the liver, kidney parameters. Even blood metabolites regulating kidney health regulator such as creatinine, BUN, uric acid and blood lipid profile cholesterol levels were unaltered in the injected set with respect to the control ones (data not shown). Similarly histopathological analysis of all the major organs (figure 7) including brain, heart, kidney, lung, testis, spleen, stomach, uterus revealed no significant alterations; normal morphometry was maintained in control and injected set of mice. Severe toxicity symptoms could alter the regular morphometry of the organs which could be easily visualized. Only minor disarray in hepatic veins was observed in the injected mice with respect to the control ones indicating very insignificant toxicity. [44] However severe toxicity symptoms and inflammations were prevented in the treated sets with respect to control. Thus carbon dots underscored its biocompatibility through *in vitro* and *in vivo* analyses and proper utility of its unique property would bring versatile multidimensional biology based applications in near future. A detailed study on *in vivo* plant system is underway and requires much of time.

Conclusions

The light reaction of photosynthesis is oxidation reduction process in which electron carriers plays important role in modulating the system. This results in the formation of a proton gradient across the thylakoid membrane of chloroplast which brings about the conservation of energy, in the form of ATP, as these protons discharge through ATP synthase. In our studies, it was proved that CQD could promote photosynthesis by modulating the electron transfer process as it fastened the conversion of light energy to the electrical energy and finally to the chemical energy as assimilatory power (ATP and NADPH). In the presence of CQD, oxygen evolution, non cyclic photophosphorylation and ATP synthesis improved in isolated chloroplast of mung bean. In presence of CQD, electrons from water were lifted uphill, to NADP, by the combined efforts of photons absorbed by each of the two photosystems (PSI and PSII) as conformed by the activity of ferricyanide reduction (with Ferricyanide as electron acceptor in PSII) and ferredoxin-NADP reduction (with NADP as artificial electron acceptor). Side by side, in the presence of CQD, activity of ATP synthase was fastened which was confirmed by the increase ATP formation from ADP and inorganic phosphate driven by a proton gradient generated in linear electron transport of light reaction.

Acknowledgement

We would like to acknowledge DBT, ICAR-NAIP, ICAR-National Fund, ISI plan project for financial help. SM acknowledges CSIR (New Delhi) for financial support.

Notes and references

1 M. R. Badger and G. D. Price, *Journal of Experimental Botany*, 2003, **54**, 609.
2 C. Arnaud, *Chem. Eng. News Archive*, 2008, **86**, 8.
3 A. Segalla, I. Szabò, P. Costantini and G. M. Giacometti, *J. Chem. Inf. Model.*, 2005, **45**, 1691.
4 P. H. Raven, R. F. Evert and S. E. Eichhorn, *Biology of Plants New York: W.H. Freeman and Company Publishers.*, 2005, **7th ed**, 124.
5 G. Steinberg-Yfrach, J. L. Rigaud, E. N. Durantini, A. L. Moore and T. Moore, *Nature*, 1998, **392**, 479.
6. I. Nabiev, A. Rakovich, A. Sukhanova, E. Lukashev, V. Zagidullin, V. Pachenko, Y. Rakovich, J. F. Donegan, A. B. Rubin and A. O. Govorov, *Angew. Chem. Int. Ed.*, 2010, **49**, 7217.
7. A. O. Govorov and I. Carmeli, *Nano Lett.*, 2007, **7**, 620
8 P. Zrazhevskiy, M. Senaw and X. Gao, *Chem. Soc. Rev.* 2010, *39*, 4326.
9 W. Shi, Q. Wang, Y. Long, Z. Cheng, S. Chen, H. Zheng and Y. Huang, *Chem. Commun.*, 2011, **47**, 6695.
10 D. Zhou, J. D. Piper, C. Abell, D. Klenerman, D. J. Kang and L. Ying, *Chem. Commun.*, 2005, 4807.
11 Z. Wang, A. Shakya, J. Gu, S. Lian and S. Maldonado, *J. Am. Chem. Soc.*, 2013, **135**, 9275.
12 X. Michalet, F. F. Pinaud, L. A. Bentolila, J. M. Tsay, S. Doose, J. J. Li, G. Sundaresan, A. M. Wu, S. S. Gambhir and S. Weiss, *Science*, 2005, **307**, 538−544.

13 S. N. Baker and G. A. Baker, *Angew. Chem. Int. Ed.*, 2010, *49*, 6726.
14 H. Li, Z. Kang, Y. Liu and S. T. Lee, *J. Mater. Chem.*, 2012, **22**, 24230.
15 S. Chandra, P. Patra, S. H. Pathan, S. Roy, S. Mitra, A. Layek, R. Bhar, P. Pramanik and A. Goswami, *J. Mater. Chem. B*, 2013, **1**, 2375.
16 Y. P. Sun, B. Zhou, Y. Lin, W. Wang, K. A. S. Fernando, P. Pathak, M. J. Meziani, B. A. Harruff, X. Wang, H. Wang, P. G. Luo, H. Yang, M. E. Kose, B. Chen, L. M. Veca and S. Y. Xie, *J. Am. Chem. Soc.*, 2006, **128**, 7756.
17 S. Chandra, S. H. Pathan, S. Mitra, B. H. Modha, A. Goswami and P. Pramanik, *RSC Adv.*, 2012, **2**, 3602.
18 L. Cao, X. Wang, M. J. Meziani, F. Lu, H. Wang, P. G. Luo, Y. Lin, B. A. Harruff, L. M. Veca, D. Murray, S. Y. Xie and Y. P. Sun, *J. Am. Chem. Soc.*, 2007, **129**, 11318.
19 Q. L. Zhao, Z. L. Zhang, B. H. Huang, J. Peng, M. Zhang and D. W. Pang, *Chem. Commun.*, 2008, 5116.
20 S. Chandra, P. Das, S. Bag, D. Laha and P. Pramanik, *Nanoscale*, 2011, **3**, 1533.
21 S. Zhu, Q. Meng, L. Wang, J. Zhang, Y. Song, H. Jin, K. Zhang, H. Sun, H. Wang and B. Yang, *Angew. Chem. Int. Ed.*, 2013, **52**, 3953.
22 S. Chandra, S. Mitra, D. Laha, S. Bag, P. Das, A. Goswami and P. Pramanik, *Chem. Commun.*, 2011, **47**, 8587.
23 F. Wang, S. Pang, L. Wang, Q. Li, M. Kreiter and C. Y. Liu, *Chem. Mater.*, 2010, **22**, 4528.
24 (a) L. Cao, S. Sahu, P. Anilkumar, C. E. Bunker, J. Xu, K. A. S. Fernando, P. Wang, E. A. Guliants, K. N. Tackett and Y. P. Sun, *J. Am. Chem. Soc.*, 2011, *133*, 4754. (b) S. Mitra, S. Chandra, P. Patra, P. Pramanik and A. Goswami, *J. Mater. Chem.* 2011, **21**, 17638.
25 Z. Ma, Y. L. Zhang, L. Wang, H. Ming, H. Li, X. Zhang, F. Wang, Y. Liu, Z. Kang and S. T. Lee, *ACS Appl. Mater. Interfaces.*, 2013, **5**, 5080.
26 L. Sun, L. Hammarström, B. Åkermark and S. Styring, *Chem. Soc. Rev.*, 2001, *30*, 36; J. W. Lee and E. Greenbaum, *J. Phys. Chem. B*, 2004, **108**, 3935.
27 H. Liu, T. Ye and C. Mao, *Angew. Chem. Int. Ed.*, 2007, *46*, 6473.
28 B. Mohanty, A. K. Verma, P. Claesson and H. B. Bohidar, *Nanotechnology*, 2007, **18**, 445102.
29 (a) Y. Yang, J. Cui, M. Zheng, C. Hu, S. Tan, Y. Xiao, Q. Yang and Y. Liu, *Chem. Commun.*, 2012, **48**, 380. (b) F. Jiang, D. Chen, R. Li, Y. Wang, G. Zhang, S. Li, J. Zheng, N. Huang, Y. Gu, C. Wang and C. Shu, *Nanoscale*, 2013, **5**, 1137.
30 Z. Lin, W. Xue, H. Chen and J. M. Lin, *Chem. Commun.*, 2012, **48**, 1051.
31 S. Zhu, J. Zhang, C. Qiao, S. Tang, Y. Li, W. Yuan, B. Li, L. Tian, F. Liu, R. Hu, H. Gao, H. Wei, H. Zhang, H. Sun and B. Yang, *Chem. Commun.*, 2011, **47**, 6858.
32 J. J. Shyue, M. R. D. Guire, T. Nakanishi, Y. Masuda, K. Koumoto and C. N. Sukenik, *Langmuir* 2004, **20**, 8693.
33 J. S. Park, S. M. Cho, W. J. Kim, J. Park and P. J. Yoo, *ACS Appl. Mater. Interfaces* 2011, **3**, 360.
34 P. Luo, Z. Ji, C. Li and G. Shi, *Nanoscale*, 2013, **5**, 7361.
35 S. Mitra, S. Chandra, T. Kundu, R. Banerjee, P. Pramanik and A. Goswami, *RSC Adv.*, 2012, **2**, 12129.
36 D. Zhou, L. Ying, X. Hong, E. A. Hall, C. Abell and D. Klenerman, *Langmuir* 2008, **24**, 1659.
37 R. Freeman and I. Willner, *Chem. Soc. Rev.*, 2012, **41**, 4067.
38 A. Jaiswal, S. S. Ghosh and A. Chattopadhyay, *Chem. Commun.*, 2012, **48**, 407.
39 (a) G. Applerot, J. Lellouche, A. Lipovsky, Y. Nitzan, R. Lubart, A. Gedanken and E. Banin, *Small*, 2012, **8**, 3326. (b) J. H. Li, X. R. Liu, Y. Zheng, F. F. Tian, G. Y. Zhao, Q. L. Y. Yu, F. L. Jiang and Y. Liu, *Toxicol. Res.*, 2012, **1**, 137.
40 R. Barr and F. L. Crane, *Plant Physiol.* 1981, **67**, 1190.
41 B. C. Gerwick, G. J. Williams and E. G. Uribe, *Plant Physiol.*, 1977, **60**, 430.
42 S. Jana and M. A. Choudhuri, *J. Aquat. Plant Manage.*, 1980, **18**, 30.
43 L. Taiz and E. Zeiger, *Plant Physiology* 2006, **4th edition**, Snauer Associates Inc., Publishers, Massachusetts.
44 S. Mitra, B. Subia, P. Patra, S. Chandra, N. Debnath, S. Das, R. Banerjee, S. C. Kundu, P. Pramanik and A. Goswami, *J. Mater. Chem.*, 2012, **22**, 24145.